Smith, S. G., Lewis, M., Aschaffenburg, R., Fenna, R. E., Wilson, I. A., Sundaralingam, M., Stuart, D. I., & Phillips, D. C. (1987) *Biochem. J. 242*, 353–360.
Stuart, D. I., Acharya, K. R., Walker, N. P. C., Smith, S. G., Lewis, M., & Phillips, D. C. (1986) *Nature (London) 324*, 84–87.
Warme, P. K., Momany, F. A., Rumball, S. V., Tuttle, R. W., & Scheraga, H. A. (1974) *Biochemistry 13*, 768–782.
Wien, R. W., Morrisett, J. D., & McConnell, H. M. (1972) *Biochemistry 11*, 3707–3716.
Wuthrich, K. (1986) *NMR of Proteins and Nucleic Acids*, Wiley, New York.

NMR Studies of Complex Formation between the Modified Oligonucleotide d(T*TCTGT) Covalently Linked to an Acridine Derivative and Its Complementary Sequence d(GCACAGAA)

G. Lancelot,* J.-L. Guesnet, U. Asseline, and N. T. Thuong
Centre de Biophysique Moléculaire, CNRS, 45071 Orléans Cedex 2, France
Received April 30, 1987; Revised Manuscript Received October 8, 1987

ABSTRACT: The oligodeoxynucleotide d(TTCTGT) was covalently attached to the 9-amino group of 2-methoxy-6-chloro-9-aminoacridine (Acr) through its 3′-phosphate via a pentamethylene linker (m_5). In order to avoid its hydrolysis by nucleases inside the cell, one of its phosphates (TpT) was substituted with a neopentyl group. Complex formation between each of the two purified isomers and the complementary strand d(GCACAGAA) was investigated by nuclear magnetic resonance. The COSY and NOESY connectivities allowed us to assign all the proton resonances of the bases, the sugars (except the overlapping 5′–5″ resonances), the acridine, and the pentamethylene chain. Structural information derived from the relative intensity of COSY and NOESY maps revealed that the duplex d(T*TCTGT)·d(GCACAGAA) adopts a B-type conformation and that the deoxyriboses preferentially adopt a 2′-endo conformation. The NOE connectivities observed between the protons of the bases or the sugars and the protons of the dye show the intercalation of the acridine between the base pairs. NOE connectivities as well as imino proton resonances show that, at room temperature, the C_7 base and the G_8 base belonging to two different duplexes are paired. The pseudoaxial and pseudoequatorial isomers were assigned, and the differences in stability of their complex with the complementary strand are discussed.

The regulation of gene expression in both procaryotes and eucaryotes requires molecules with a high specificity and strong affinity for a nucleic acid base sequence. These biological processes are usually controlled by specific proteins which are able to recognize a base sequence or a nucleic acid local structure (Hélène & Lancelot, 1982).

We have recently synthesized a new family of molecules which are aimed at selectively recognizing nucleic acid base sequences (Asseline et al., 1984a,b). These molecules involve an oligodeoxynucleotide covalently linked to an intercalating dye. The binding of the oligonucleotide to its complementary sequence is a highly specific process governed by stacking interactions between base pairs and by hydrogen-bond formation between complementary bases. The intercalating agent should provide an additional binding energy, through stacking interactions with the base pairs, which is expected to stabilize the specific complex. The intercalating dye was chosen in such a way as to be nonspecific with respect to base or base pair interaction.

Hence, a derivative of 9-aminoacridine (2-methoxy-6-chloro-9-aminoacridine) was covalently attached to the 3′-terminal residue of a deoxyoligonucleotide via a pentamethylene bridge: d(TTCTGT)m_5Acr.

Absorption studies showed that the presence of the dye strongly stabilized the complexes formed by the oligonucleotides with their target sequence (Asseline et al., 1984a,b).

We undertook a nuclear magnetic resonance investigation of the interaction of d(T*TCTGT)m_5Acr[1] with its complementary sequence. The conformation of the duplex is clearly shown. We have already demonstrated (Lancelot et al., 1985, 1986) that oligonucleotides linked to an acridine derivative self-associated at low temperature. In order to avoid aggregate formation, we have synthesized a complementary sequence, d(GCACAGAA), with two more bases on its 5′-terminal side than the oligonucleotide linked to the acridine derivative.

Preliminary investigations on the penetration of oligonucleotides linked to an acridine derivative across the cell membrane have shown that these oligonucleotides were rapidly hydrolyzed by nucleases inside the cell. In order to avoid such a degradation, the synthesized oligonucleotides linked to an acridine residue were substituted on one of their phosphates (TpT) by a neopentyl group (Np). The two isomers were

[1] Abbreviations: NMR, nuclear magnetic resonance; 1D and 2D, one and two dimensional; COSY DQF, double quantum filter 2D correlated spectroscopy; NOE, nuclear Overhauser effect; NOESY, 2D NOE spectroscopy; $1\bar{3}3\bar{1}$, composite pulse of excitation with alternated phase; d(T*TCTGT)m_5Acr, deoxyribohexanucleotide d(TTCTGT) linked on its 3′-terminal phosphate to the 9-amino group of 2-methoxy-6-chloro-9-aminoacridine via a pentamethylene linker and substituted on its TpT phosphate with a neopentyl group; Acr, 2-methoxy-6-chloro-9-aminoacridine; m_5, pentamethylene chain, $-(CH_2)_5-$; Np, neopentyl group; Aro, H_6 or H_8 proton of base A, T, G, or C; $H_{1'}(5')$ and $H_{2'}(5')$, $H_{1'}$ and $H_{2'}$ proton of the 5′ neighboring nucleotide.

0006-2960/88/0427-1265$01.50/0

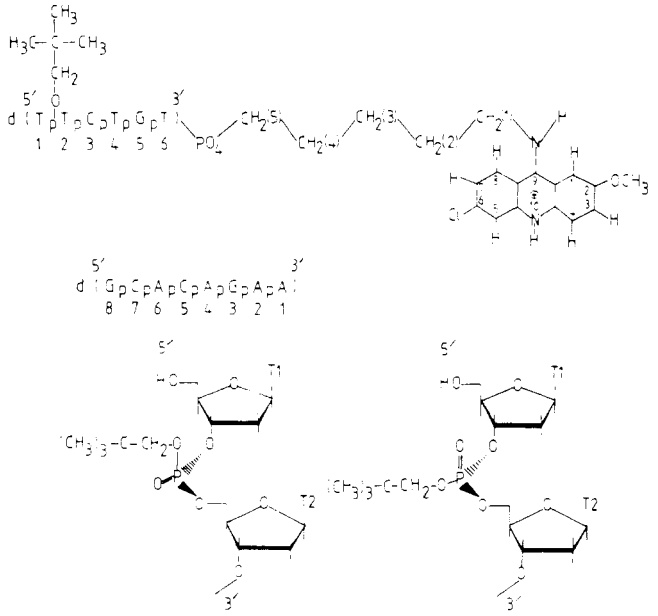

FIGURE 1: (Top) Structures of the two oligodeoxyribonucleotides d(T*TCTGT)m_5Acr and d(GCACAGAA). The phosphate linking the two thymines T_1 and T_2 is substituted by a neopentyl group, and the two resulting isomers are called I and II. The sequence d-(GCACAGAA) was numbered from its 3′-terminal residue. (Bottom) Diastereoisomers of the oligonucleotide neopentyl phosphate: (right) pseudoequatorial; (left) pseudoaxial.

purified, and it has been shown that their behavior with nuclease S_1 was different. NMR studies allowed us to assign these two compounds and to show that the acridine rings underwent stacking interactions with the base pairs in the duplex structure formed by d(TTCTGT) and its complementary sequence.

Experimental Procedures

Covalent attachment of 2-methoxy-6-chloro-9-aminoacridine to the oligodeoxynucleotides involved a chain of five methylene groups linking the 3′-phosphate of the hexanucleotides to the 9-amino group of acridine. The first internucleotide phosphate at the 5′-end of the two hexanucleotides 5′-Tp($CH_2C(CH_3)_3$)TpCpTpGpTp(CH_2)$_5$Acr (isomers I and II) was esterified by a neopentyl group in the pseudoaxial or pseudoequatorial position. The oligonucleotides have been synthesized via the phosphotriester method in solution (Stawinski et al., 1977; Thuong et al., 1981; Asseline et al., 1986a) from each pure isomer of the neopentylated dithymidylate (Asseline et al., 1986b) and were abbreviated to d(T*TCTGT)m_5Acr (Figure 1).

After the dearylation carried out by use of the benzohydroxamate ion in an aprotic solvent, the deprotection of nucleic bases was successfully achieved by aqueous alkali treatment in previously described conditions (Asseline et al., 1986b) as both products, the bound 9-aminoacridine and the neopentyl phosphotriester group, are stable.

The synthesis of the complementary octanucleotide 5′-d(GCACAGAA)-3′ has been realized by the usual phosphotriester method in solution (Stawinski et al., 1977; Thuong et al., 1981), and the bases have been numbered from the 3′-end (Figure 1).

All the investigated compounds were passed through a Chelex-100 column to remove paramagnetic impurities, adjusted to pH 7.0, then lyophilized, dissolved in D_2O containing 0.1 M NaCl, then lyophilized, and dissolved in 99.96% D_2O. The samples were placed in a 5-mm NMR tube, and the spectra were calibrated with respect to an internal reference of 4,4-dimethyl-4-silapentane-1-sulfonate (DSS).

NMR experiments were carried out with a Bruker AM-300 spectrometer and processed on an Aspect 3000 computer.

Proton relaxation times (T_1) were obtained by the inversion recovery method (180°–τ–90°). The T_1 relaxation times were computed by a least-squares program to fit the three parameters $I(0)$, α, and T_1 in the equation $I(t) = I(0)[1 + \alpha \exp(-t/T_1)]$.

In order to observe the low-field resonances in H_2O and to overcome the dynamic range problem arising from the intense water peak, we used the composite excitation $1\bar{3}3\bar{1}$ proposed by Hore (1983).

The NOESY data were obtained from degassed solutions contained in sealed tubes. Two-dimensional data sets for the COSY and NOESY spectra were collected in the phase-sensitive mode by the method of States et al. (1982). The experimental procedures used for COSY DQF experiments were described elsewhere (Marion & Lancelot, 1984).

Typically, 4096 complex t_2 data points were collected for each of 256 t_1 values in NOESY experiments. A mixing time of 300 ms was used. A 512 × 4096 data matrix, sampled in a 48-h experiment, was resolution-enhanced by a Gaussian window function in direction 2 and by a shifted squared "sine-bell" window function in direction 1, then Fourier transformed, and phase adjusted.

Absorption spectra were recorded with a Beckman DU-8 spectrophotometer.

Results

The interaction of the two isomers of d(T*TCTGT)m_5Acr with d(GCACAGAA) was investigated by both UV absorption and NMR spectroscopies. Figure 2 shows the changes in absorption spectra induced upon binding both complementary oligonucleotides. For each isomer, these intermolecular interactions led to both a slight red shift and a hypochromism of the acridine visible band.

Increasing the temperature of the complex formed at low temperature (Figure 2) led to a cooperative transition but a different stability for both isomers. The melting temperature for the duplex with isomer I (duplex I) was 42 °C, while that for the duplex with isomer II (duplex II) was 45 °C at a concentration of 7 mM.

The low-field region of the 300-MHz proton spectra of the mixture d(T*TCTGT)m_5Acr isomer II + d(GCACAGAA) in 0.1 M NaCl is shown in Figure 3. The mixing of both compounds induced a broadening of all the resonance lines and several upfield shifts of the aromatic resonances for both isomers. These facts indicate the formation of a duplex.

Assignment of Resonances. The use of the sequential NOE method for the assignment of nonexchangeable resonances in nucleic acids has been described elsewhere (Hare et al., 1983; Scheek et al., 1983, 1984; Feigon et al., 1983, 1984; Weiss et al., 1984; Wemmer et al., 1984, 1985; Guittet et al., 1984; Broido et al., 1984) and will not be repeated here.

Figures 4–7 present four parts of the NOESY map of the mixture d(T*TCTGT)m_5Acr isomer I + d(GCACAGAA) (2.5 mM:2.5 mM) at 24 °C. Except for the terminal residues, all the H_8 or H_6 resonances presented two NOE effects with the $H_{1'}$ resonances (Figure 4). The examination of the computed interproton distances, for a B-DNA model, shows that Aro(n)–$H_{1'}$(n) = 3.88 Å is quite similar in comparison with Aro(n)–$H_{1'}$(5′) = 3.63 Å. By using this fact and noticing that the 5′-terminal residue resonance presents an NOE effect with a single $H_{1'}$ resonance (its own $H_{1'}$), all the H_8 and H_6 resonances as well as the $H_{1'}$ resonances were sequentially assigned for both oligonucleotides. The same procedure was repeated

Table I: Assignment of Proton Resonances in the Mini Double Helix d(T*TCTGT)m_5Acr Isomer I + d(GCACAGAA) (2.5 mM:2.5 mM) in 0.1 M NaCl, pH 7.0 at 24 °C

	H_8	H_6	H_5	CH_3	H_2	$H_{1'}$	$H_{2'}$	$H_{2''}$	$H_{3'}$	$H_{4'}$
A_1	8.13				7.77	6.18	2.41	2.59	4.67	4.18
A_2	8.01				7.68	5.95	2.53	2.74	4.95	4.30
G_3	7.63					5.26	2.47	2.47	4.90	4.07
A_4	8.08				7.52	5.78	2.59	2.72	4.98	4.28
C_5		7.21	5.88			5.34	2.20	2.20	4.72	4.08
A_6	8.30				7.77	6.05	2.67	2.90	4.88	4.40
C_7		7.30	5.70			5.20	2.22	2.65	4.88	4.10
G_8	7.45					5.77	2.27	2.45		4.28
T_1		7.41		1.63		6.05	2.35	2.45	5.01	4.20
T_2		7.44		1.81		6.17	2.39	2.63	4.87	4.38
C_3		7.70	5.75			6.03	2.18	2.56	4.85	4.21
T_4		7.37		1.67		5.67	2.15	2.45	4.87	4.13
G_5	7.85					5.87	2.62		4.96	4.31
T_6		7.02		1.27						

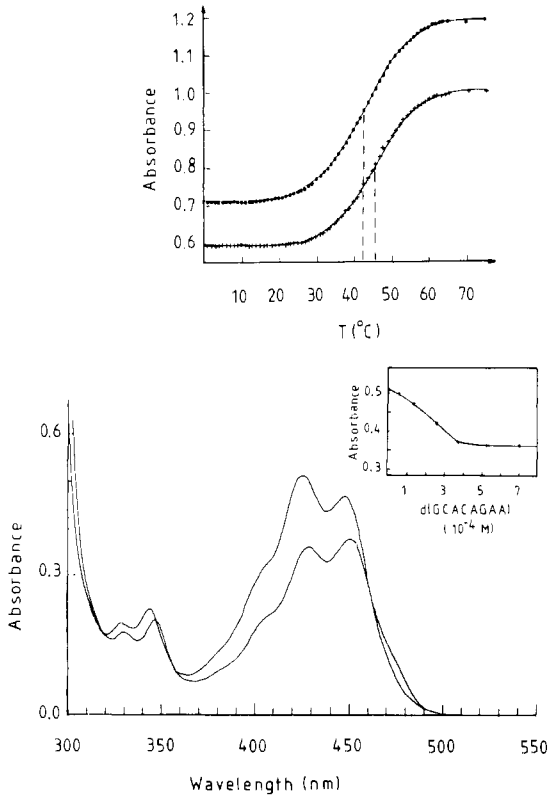

FIGURE 2: (Bottom) Change in absorption spectra of (T*TCTGT)m_5Acr isomer I (6.62×10^{-4} M) upon addition of d(GCACAGAA) (6.62×10^{-4} M) in H_2O–1 M NaCl, pH 7.0 at 20 °C. (Insert) Variation of absorbance at 424 nm of d(T*TCTGT)m_5Acr isomer I (4.0×10^{-4} M) versus the concentration of d(GCACAGAA) in H_2O–1 M NaCl pH 7.0 at 20 °C. (Top) Melting curves measured at 425 nm for complexes (1:1) of d(T*TCTGT)m_5Acr isomer I (+) or isomer II (○) and d(GCACAGAA) (7 mM) in H_2O–1 M NaCl pH 7.0.

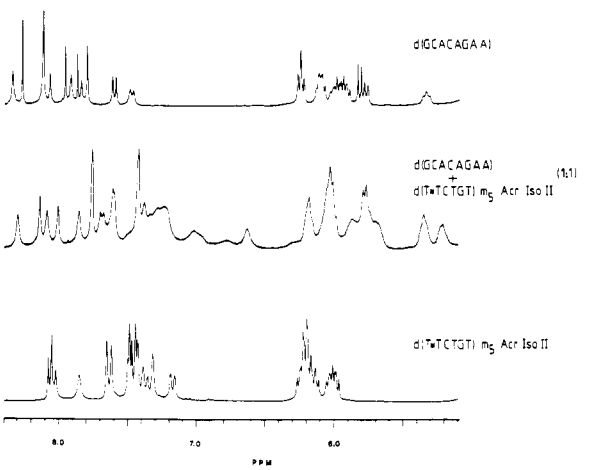

FIGURE 3: The 300-MHz ^1H NMR spectrum of 2 mM d(GCACAGAA) (upper spectrum), 2 mM d(T*TCTGT)m_5Acr isomer II (lower spectrum), and their 1:1 complex (middle spectrum) in 0.1 M NaCl, pH 7.0 at 24 °C.

with the NOE effects between the aromatic H_8/H_6 protons and the $H_{2'}/H_{2''}$ sugar protons (Figure 5). These assignments were confirmed from their NOE connectivities with the $H_{1'}$ proton belonging to the same residue. We identified the $H_{3'}$ and $H_{4'}$ sugar protons by their proximity to the aromatic protons and other protons of the sugar. The $H_{5'}/H_{5''}$ resonances of 5′-terminal residues are easy to attribute, since their separation from any phosphate group induced an upfield shift of about 0.2 ppm [$H_{5'}/H_{5''}(T_1)$ = 3.68 ppm].

The H_2 resonances of adenine, recognizable by their long T_1 relaxation time, show some NOE effects with the $H_{1'}$ proton of adenine A_1, A_6 [$\delta(H_2)$ = 7.77 ppm], and A_4 [$\delta(H_2)$ = 7.52 ppm] (Figure 4). The fourth H_2 resonance at 7.68 ppm is overlapped at 24 °C by the resonances $H_8(G_3)$ and $H_6(C_3)$, which themselves showed strong NOE connectivities in the range 5.2–6.4 ppm with the $H_{1'}$ protons of T_2, C_3, G_3, A_4 and could not be directly assigned. By using the facts that (i) the H_2 proton of an adenine is near to the $H_{1'}$ proton of the same residue (4.40 Å) or to residues on the opposite strand, (ii) all the H_2–$H_{1'}$ observed NOEs arise with the $H_{1'}$ sugar proton of adenines, and (iii) the adenines A_1, A_2, A_4, and A_6 belong to the same strand, we have assigned the four H_2 resonances of adenines (Table I).

The assignments of the H_5 protons of cytosines and of the CH_3 protons of thymines were obtained from their NOE connectivities with their neighboring protons (Figures 4 and 5). These assignments were confirmed with the COSY map. The connectivities between H_5 and $H_{1'}$ protons of cytosine moieties were also observed (Figure 4). Moreover, the observed interbase NOE effects between neighboring aromatic protons [$H_8(A_2)$–$H_8(G_3)$; $H_8(G_3)$–$H_8(A_4)$; ...] (Figure 6), which reflected the proximity of adjacent bases, were in agreement with the assignments already made.

Conformation of the Duplex. It has been already computed that in right-handed DNA the H_8 or H_6 proton of a base is close to the $H_{1'}$ sugar proton of its 5′-neighboring nucleotide (Feigon et al., 1983). In contrast, the opposite situation is observed in left-handed DNA (Fazakerley et al., 1985; Lancelot & Thuong, 1986).

From the assignment made above and the observation that the nearest $H_{1'}$ proton of each H_8 or H_6 proton always belonged to the 5′-neighboring nucleotide, we conclude that the duplex

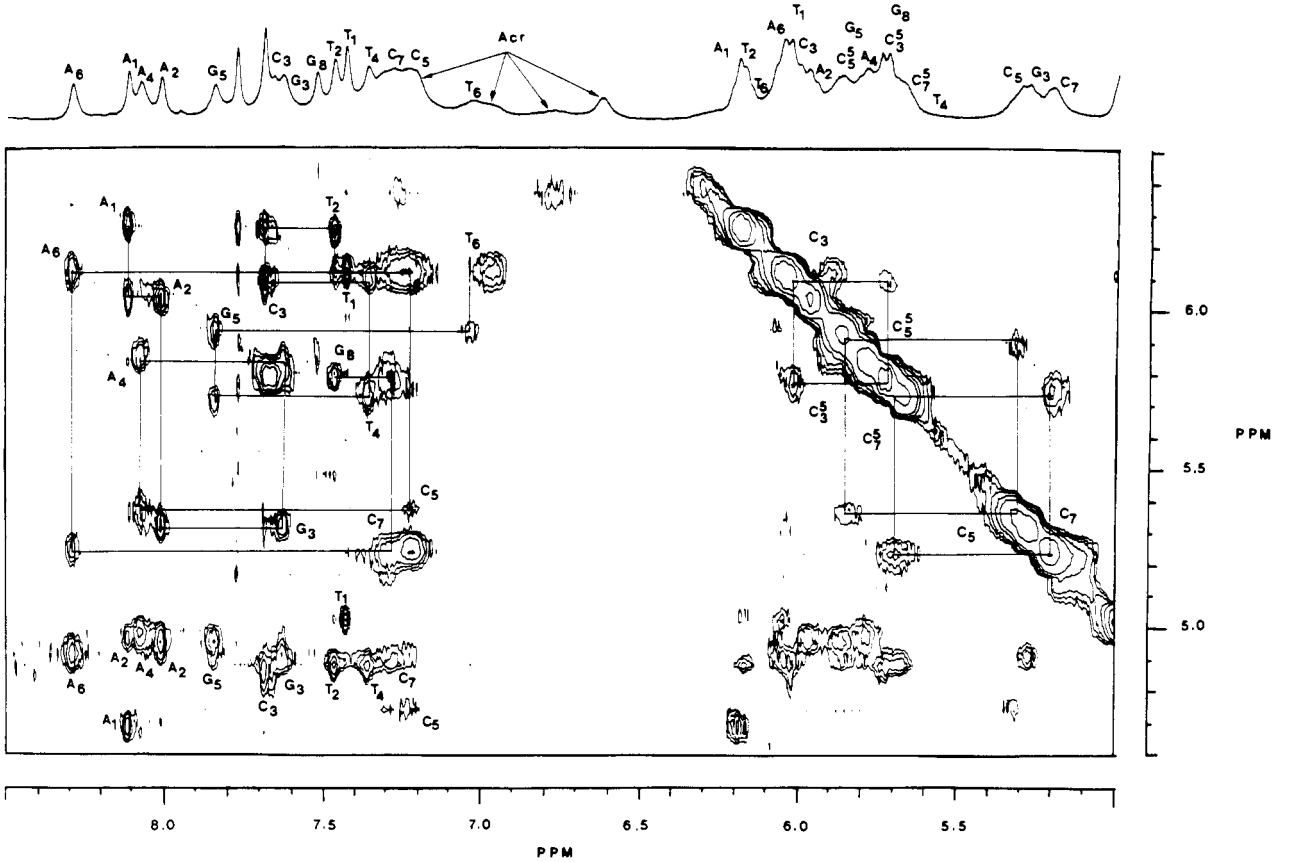

FIGURE 4: Expansion of the aromatic to the $H_{1'}$ proton region of the NOESY spectrum of d(T*TCTGT)m_5Acr isomer I + d(GCACAGAA) at 24 °C (2.5 mM:2.5 mM) in 0.1 M NaCl, pH 7.0. The sequential assignment of the two strands is indicated with a solid line (H_6–$H_{1'}$ or H_8–$H_{1'}$ NOE). The labeled connectivities correspond to the observed cross-peak between the H_8 or H_6 resonances of the base and their own $H_{1'}$ resonances. The connectivities between aromatic resonances and $H_{3'}$ are also shown. The cross-peaks near to the diagonal in the region (5.2–6.2 ppm) are indicative of the proximity of the H_5 protons of cytosine to their own $H_{1'}$. Several NOEs are also observed between the aromatic protons of the acridine (Acr) and the H_6/H_8 of the bases or $H_{1'}$ of sugars (see text).

adopts a right-handed helical structure.

This conclusion is supported by the fact that the connectivity of H_6 or H_8 with the $H_{2''}$ belonging to the 5′-neighboring nucleotide [H_6– or $H_8(n)$–$H_{2''}(5')$] was stronger than the connectivity of H_6 or H_8 with $H_{2'}(5')$. In a right-handed B-conformation, H_6 or H_8 protons are closer to the H_5 proton of the 3′-neighboring cytosine or to the CH_3 of the 3′-neighboring thymine (3.8–3.6 Å) than the corresponding proton of the 5′-neighboring base (6.7 Å) whose NOE connection cannot be observed [see, for example, the observed NOE effects in d(ATATGCAAT); Feigon et al., 1983]. As a matter of fact, an NOE effect was observed for the protons $H_6(T_1)$–$CH_3(T_2)$, $H_6(C_3)$–$CH_3(T_4)$, and $H_8(G_5)$–$CH_3(T_6)$.

Information about sugar geometry can be obtained from the scalar coupling constants observed between the protons $H_{1'}$, $H_{2'}$, $H_{2''}$, and $H_{3'}$. It has been already shown (Govil et al., 1985; Lancelot & Thuong, 1986) that the simple analysis of the intensity of the connectivities in a COSY map allows us to differenciate between the strong (large cross-peaks) and weak (small cross-peaks) coupling constants. We can then predict that the coupled system $H_{1'}$, $H_{2'}$, $H_{2''}$, and $H_{3'}$ will present three cross-peaks with very different characteristics for 2′-endo or 3′-endo conformation. In the 2′-endo conformations, the $H_{1'}$ proton will present two cross-peaks with the $H_{2'}$ and $H_{2''}$ protons ($J_{1'2'}$ = 10.1 Hz and $J_{1'2''}$ = 5.5 Hz), and the $H_{3'}$ proton will present only one cross-peak with the $H_{2'}$ proton ($J_{2'3'}$ = 5.5 Hz, $J_{2''3'}$ = 0.1 Hz). In the 3′-endo conformations, the $H_{1'}$ protons will present only one cross-peak (or additionally a very weak second cross peak) with $H_{2''}$ protons ($J_{1'2'}$ = 0.1 Hz, $J_{1'2''}$ = 7.4 Hz), and the $H_{3'}$ proton will present two cross-peaks with the $H_{2'}/H_{2''}$ protons ($J_{2'3'}$ = 4.9 Hz, $J_{2''3'}$ = 11.0 Hz).

An analysis of the COSY DQF map shows that each $H_{1'}$ proton presents two connectivities of slightly different intensity with the $H_{2'}/H_{2''}$ protons. Moreover, the $H_{2'}$ resonances (corresponding to the stronger connectivity $H_{1'}$–$H_{2'}/H_{2''}$) were connected to the $H_{3'}$ resonance while the $H_{2''}$ resonances were not connected. Therefore, we conclude that the sugar conformation is predominantly 2′-endo in the duplex structure. We can remark that all the $H_{2'}$ resonances were observed at higher field than the $H_{2''}$ resonances (Table I). The NOE connectivities $H_{2''}$–$H_{1'}$ obtained for mixing times equal or less than 300 ms were stronger than that observed between the $H_{2'}$ and $H_{1'}$ protons, indicating that the distance $H_{2''}$–$H_{1'}$ is smaller than the distance $H_{2'}$–$H_{1'}$ as expected in the ^2E conformations.

Some weaker NOE effects were also observed between the protons H_6 and H_8 of the neighboring bases: $H_8(A_2)$–$H_8(G_3)$, $H_8(G_3)$–$H_8(A_4)$, $H_6(C_5)$–$H_8(A_6)$, $H_6(T_2)$–$H_6(C_3)$, and H_6-(C_3)–$H_6(T_4)$. These weak connections correspond to computed distances of about 5 Å in the classical A or B conformation. All these data are indicative of the formation of a duplex structure, with stacked bases in a conformation belonging to the B family with 2′-endo sugars.

Intercalation of the Acridine Derivative. The H_7 and H_8 protons of the acridine derivative were assigned [$\delta(H_7)$ = 6.63 ppm and $\delta(H_8)$ = 7.28 ppm] by use of their connectivities observed on COSY and NOESY spectra and the assignment already made for the same acridine derivative linked to an oligothymidylate (Lancelot et al., 1985) or to a tetranucleotide (Lancelot & Thuong, 1986). The so-called H_D protons cor-

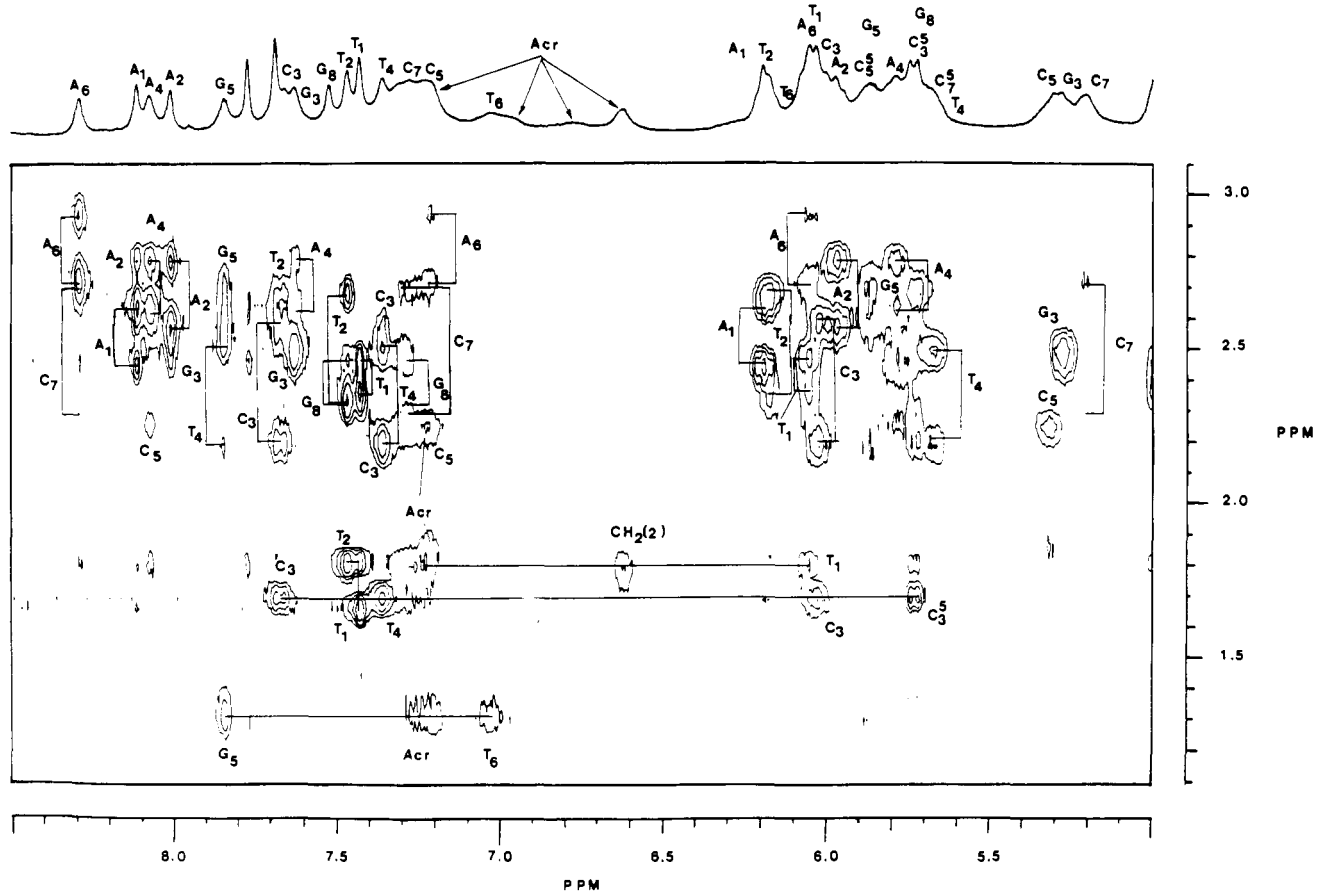

FIGURE 5: Expansion of the aromatic to the $H_{2'}/H_{2''}$ proton region of the NOESY spectrum of d(T*TCTGT)m_5Acr isomer I + d(GCACAGAA) (2.5 mM:2.5 mM) at 24 °C in 0.1 M NaCl, pH 7.0. The connectivities $H_{2'}/H_{2''}$–H_6/H_8 and $H_{2'}/H_{2''}$–$H_{1'}$ are labeled as well as the connectivities between the methyl groups of T_1, T_2, T_4, and T_6 and the H_6/H_8 protons of their own bases or their 5′ neighbor. The aromatic resonances of the acridine dye show some connectivities with the methylene resonances of the linker and the CH_3 resonance of thymine T_6.

respond to the H_1, H_3, H_4, and H_5 protons, which could not be individually assigned in the complex. The characteristic singlet of the 2-methoxy group was found at about 3.7 ppm. The protons of the methylene chain were assigned from their NOE connectivities between themselves and with the aromatic protons of acridine by assuming that $CH_2(1)$ and $CH_2(2)$ rather than $CH_2(4)$ and $CH_2(5)$ should present NOE connectivities with the protons of the acridine rings (Figures 6 and 7). They were located at 3.56, 1.73, 1.46, 1.62, and 3.32 ppm for $CH_2(1)$, $CH_2(2)$, $CH_2(3)$, $CH_2(4)$, and $CH_2(5)$, respectively. Moreover, the $CH_2(1)$, $CH_2(2)$, and $CH_2(5)$ groups showed an NOE effet with the H_7 acridine proton (Figures 5 and 7) while the $CH_2(1)$ group presented a connectivity with another proton of acridine (Figure 7).

Figures 4–6 show the NOE effects observed between protons of the acridine derivative and protons of the duplex. We observed two NOE effects located at 7.24 and 6.95 ppm between the aromatic protons of acridine H_D(Acr) and the sugar proton $H_{1'}(A_6)$ and the methyl group $CH_3(T_6)$, one 1D NOE connectivity between the proton of the acridine at 6.98 ppm and the $H_{1'}$ sugar proton of the cystosine C_7, and one NOE connectivity between the proton of the acridine located at 6.63 ppm and the proton H_6 of the cytosine C_7. The 2-methoxy group never exhibited any NOE cross-peaks with the protons of nucleotides. This can be due to the combined effect of the rotation of the OCH_3 group about the C–O bond, which induces several surroundings of the methyl group, and of the short correlation time of the methyl group.

The NOE effects observed between protons of the acridine derivative and protons of the base T_6 or protons of the sugar A_6 point out the proximity of the drug to the T_6-A_6 base pair. This conclusion is supported by the fact that the chemical shift of $CH_3(T_6)$ was considerably upfield shifted [δ(duplex at 22 °C) − δ(monomer at 90 °C) = 0.65 ppm], whereas the ring current calculation (duplex without acridine in the B form) predicts a value less than 0.1 ppm. This unexpected upfield shift could be attributed to the ring current effect of the acridine derivative, which can reach 1.8 ppm (Barbet et al., 1976). Moreover, the connectivity between $H_{1'}(G_5)$ and $H_6(T_6)$ is particularly weak. This remoteness of G_5 and T_6 could be explained by the intercalation of acridine between both G_5-C_5 and T_6-A_6 base pairs, as already observed for intercalated dye (Reid et al., 1983; Brown et al., 1984; Lancelot et al., 1986). Netherless, it cannot be excluded that these weak connectivities were caused by a distortion of the helix resulting from acridine binding modes other than the intercalation presented in model I (Figure 9). The large broadening of the aromatic proton of acridine was tentatively explained by the exchange between both structures shown in Figure 9. The fact that the NOESY map showed (Figure 6) more connectivities than expected supports this assumption.

Identification of Isomers. The resonance lines of the CH_3(Np) and of the CH_2(Np) were located at 0.85 and at 3.75 ppm, respectively, and were shown to be insensitive to temperature.

The NOESY map of duplex I presented NOE effects between CH_2(Np) and $CH_3(T_2)$, $H_{2'}/H_{2''}$, and $H_{4'}(T_1)$, while we never observed any NOE effects with the neopentyl group in the duplex II.

The examination of molecular Corey–Pauling–Koltren (CPK) models of the isomers showed that in the pseudoaxial isomer the CH_2 protons of the neopentyl group are near to the

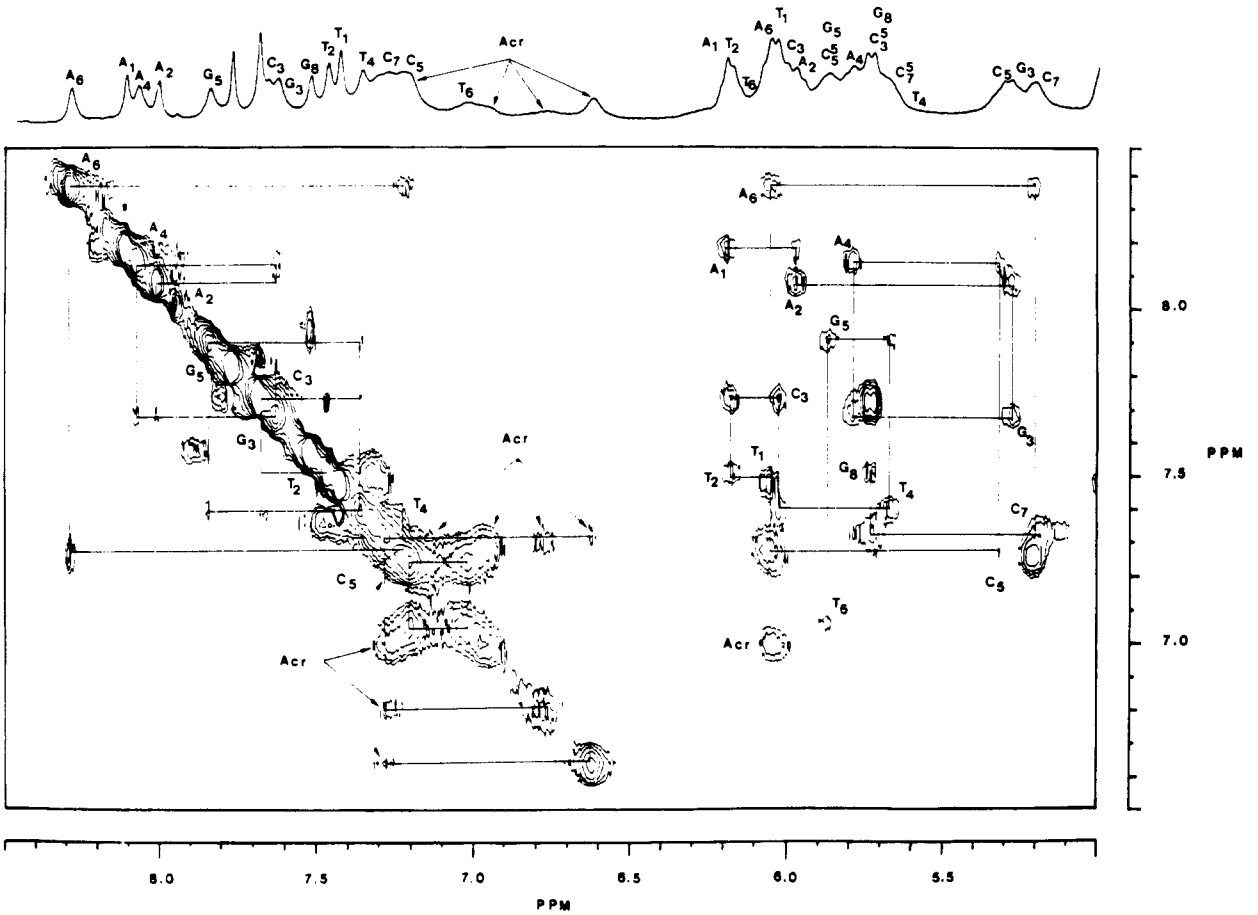

FIGURE 6: Expansion of the aromatic to the aromatic proton region of the NOESY spectrum of d(T*TCTGT)m_5Acr isomer I + d(GCACAGAA) (2.5 mM:2.5 mM) at 24 °C in 0.1 M NaCl, pH 7.0. Cross-peaks between protons of neighboring bases (H_6–H_8/H_6–H_8 or H_2–H_2), between acridine protons, and between acridine protons and H_2 of adenine are shown. The sequential assignment of the two strands is shown on the right (connectivity H_6– or H_8–$H_{1'}$).

$H_{2'}$, $H_{2''}$, $H_{3'}$, $H_{5'}$, and $H_{5''}$ protons of T_1 and the CH_3 group of T_2, whereas in the pseudoequatorial isomer the CH_2 protons of the neopentyl group are near the $H_{5'}$ and $H_{5''}$ protons of T_2. We conclude that the so-called isomer I has a pseudoaxial configuration and isomer II a pseudoequatorial configuration (Figure 1).

Exchangeable Proton Resonances. Figure 8 shows the low-field region of the spectrum of the mixture d-(T*TCTGT)m_5Acr isomer II + d(GCACAGAA) (2.5 mM:2.5 mM) at room and at low temperature. At 22 °C, three strong resonances at 13.83, 12.62, and 12.39 ppm were observed as well as less intense resonances at 13.03 ppm and overlapped resonances in the range 12.2–12.7 ppm.

Lowering the temperature led to the appearance of more separated resonances at 12.43, 12.54, 12.66, 12.73, 13.12, and 13.19 ppm between 10 and 5 °C while one more resonance arose at 12.28 ppm below 4 °C.

1D NOE experiments showed that presaturation of the resonance at 13.83 ppm led to an NOE effect on the H_2 resonance of adenine at 7.61 ppm, while the resonances in the range 12.5–12.8 ppm showed two NOE effects with the H_2 protons of adenines at 7.78 ppm. The proximity of the NH resonances as well as the lack of selectivity in the irradiation prevented us from assigning separately the N_3H resonances of the thymines. Moreover, the resonance at 12.54 ppm showed an NOE effect with the amino resonance of a cytosine at 8.43 ppm.

Autoassociation. A simple model of pairing leaves C_7 and G_8 unpaired. The NOE effect observed between the $H_{1'}(G_8)$ and the $H_6(C_7)$ of these two residues demonstrates the proximity of these residues. We suggest that this conformation corresponds to the formation of duplex dimer in which the guanine G_8 is paired with the cytosine C_7.

Lowering the temperature of a 2 mM sample of d-(T*TCTGT)m_5Acr isomer I (or isomer II) in D_2O, 0.1 M NaCl, led to several upfield shifts of the aromatic protons of the bases and of the acridine. Although these upfield shifts indicated a stacking between the bases and the acridine, we never observed any NOE connectivities between the acridine protons and protons of either bases or sugars. NOESY spectra of both isomers recorded with a mixing time of 300 ms showed connectivities between the H_6 or H_8 protons of bases and their own $H_{1'}$ sugar protons but not with the $H_{1'}$ protons of their neighboring residues. We conclude that both isomers of the oligonucleotide d(T*TCTGT)m_5Acr adopt a random coil structure where the bases are far from their neighboring residue.

The low-field region of the proton NMR spectra in H_2O/D_2O (4:1) (Figure 8) showed three imino resonances at 12.90 ppm (2 protons), 11.31 ppm (1 proton), and 11.17 ppm (2 protons) as well as two amino resonances at 8.82 and 9.27 ppm.

Discussion

Our data unambiguously show that, in aqueous solution at a temperature less than 45 °C, the oligodeoxynucleotides d(T*TCTGT)m_5Acr + d(GCACAGAA) form a mini right-handed double helix that adopts a B-type conformation.

Structural information is obtained from the COSY and NOESY maps. The observed NOEs prove the proximity of

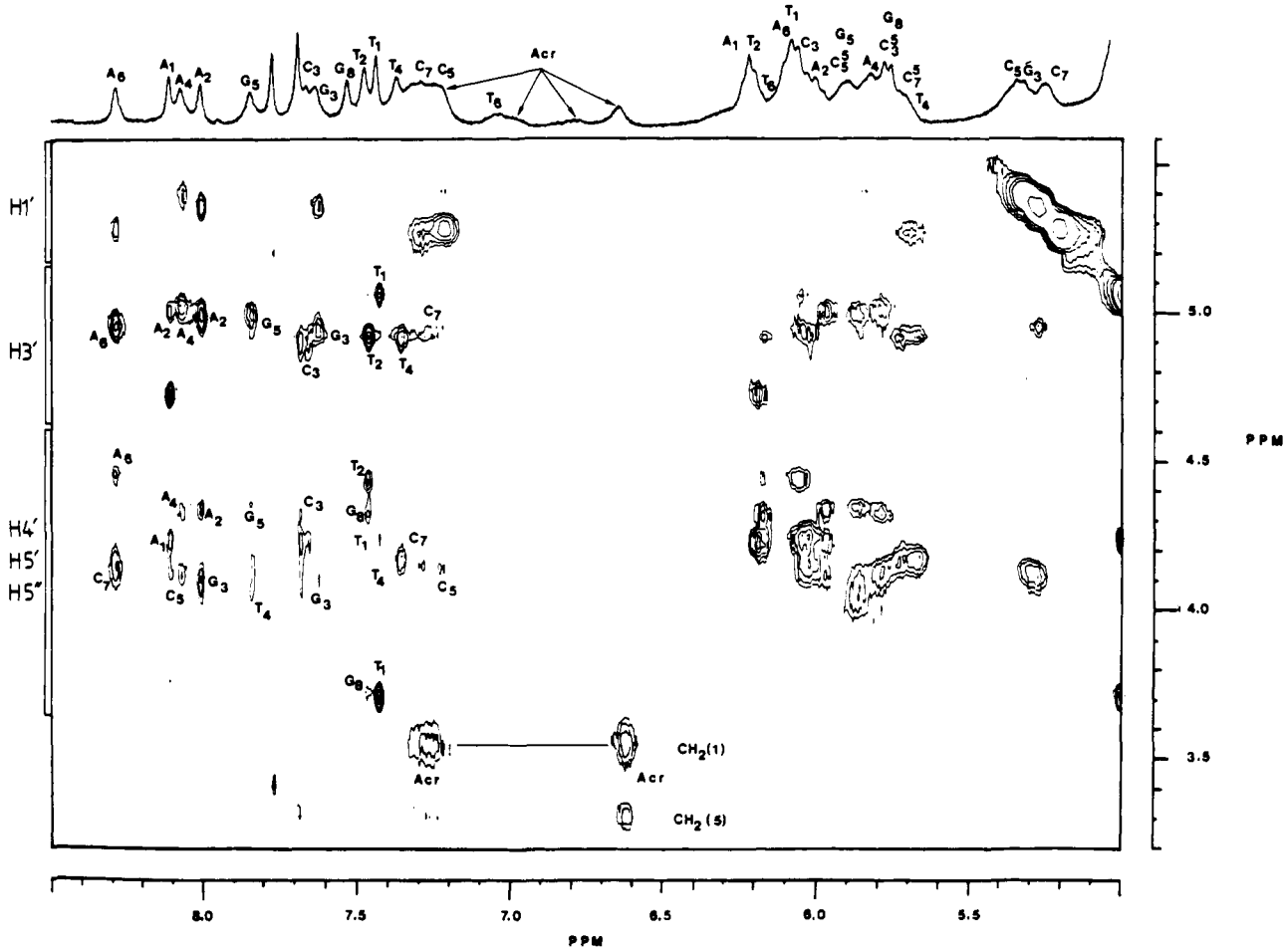

FIGURE 7: Expansion of the aromatic to the H_3-H_4-H_5-H_5" proton region of the NOESY spectrum of d(T*TCTGT)m_5Acr isomer I + d(GCACAGAA) (2.5 mM:2.5 mM) at 24 °C in 0.1 M NaCl, pH 7.0. The connectivities between the methylene resonances of the linker (labeled CH_2) and the acridine resonances are also shown.

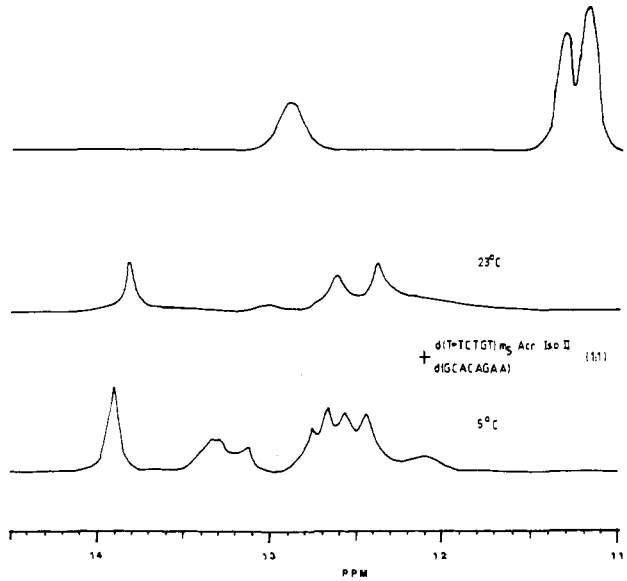

FIGURE 8: Low-field region of the ^1H NMR resonance of d-(T*TCTGT)m_5Acr isomer II + d(GCACAGAA) (2.5 mM:2.5 mM), pH 7.0 at 5 °C (bottom spectrum) and at 23 °C (middle spectrum) and of d(T*TCTGT)m_5Acr isomer II (2 mM) at 7 °C (top spectrum).

the bases themselves and the proximity between sugars and bases while NOESY as well as the COSY spectra indicated that the sugars adopt a 2'-endo conformation.

The acridine derivative was found to be intercalated between G_5-C_5 and T_6-A_6 base pairs. Several NOEs are observed between protons of the duplex and protons of the acridine dye. The unexpected upfield shift of $H_6(C_5)$ and $CH_3(T_6)$ (0.76 and 0.65 ppm, respectively) could be due to the ring current effects of the polycyclic dye since the proton resonances H_6 and CH_3 of T_6 were predicted to be shifted upfield by less 0.1 ppm in a B-DNA model. Nevertheless, an examination of a CPK model shows that an important upfield shift of $CH_3(T_6)$ can be obtained only if the dye is stacked on the top of the T_6-A_6 base pair. Moreover, with this particular geometry, the head to tail association with another duplex will be favored by the formation of two C_7-G_8 and G_8-C_7 base pairs and by the stacking of the dye between the T_6-A_6 and the G_8-C_7 base pairs.

As a matter of fact, seven imino resonance lines were observed at low temperature as expected for a dimer of duplex involving the formation of a C_7-G_8 base pair rather than six resonance lines as provided for a complex formation with only the pairing of T_1-A_1 to T_6-A_6 bases.

This conclusion is supported by the fact that the ring current of the acridine derivative explains the significant upfield shift (0.61 ppm) observed on the H_8 resonance of G_8, while an upfield shift of only 0.04 ppm has been computed for a B-DNA model. Moreover, it was also pointed out that the H_6 and H_5 protons of C_5 were upfield shifted by 0.76 and 0.19 ppm, respectively, in the duplex while 0.65 and 0.08 ppm were respectively predicted with a B-DNA model. Such a discrepancy reflects the variation of geometry adopted by the bases (the base C_5 is surrounding by two adenines which are able to induce high upfield shifts) as compared as the B-DNA model. This cannot excluded a complex where the acridine dye is intercalated between the G_5-C_5 and the T_6-A_6 base pairs

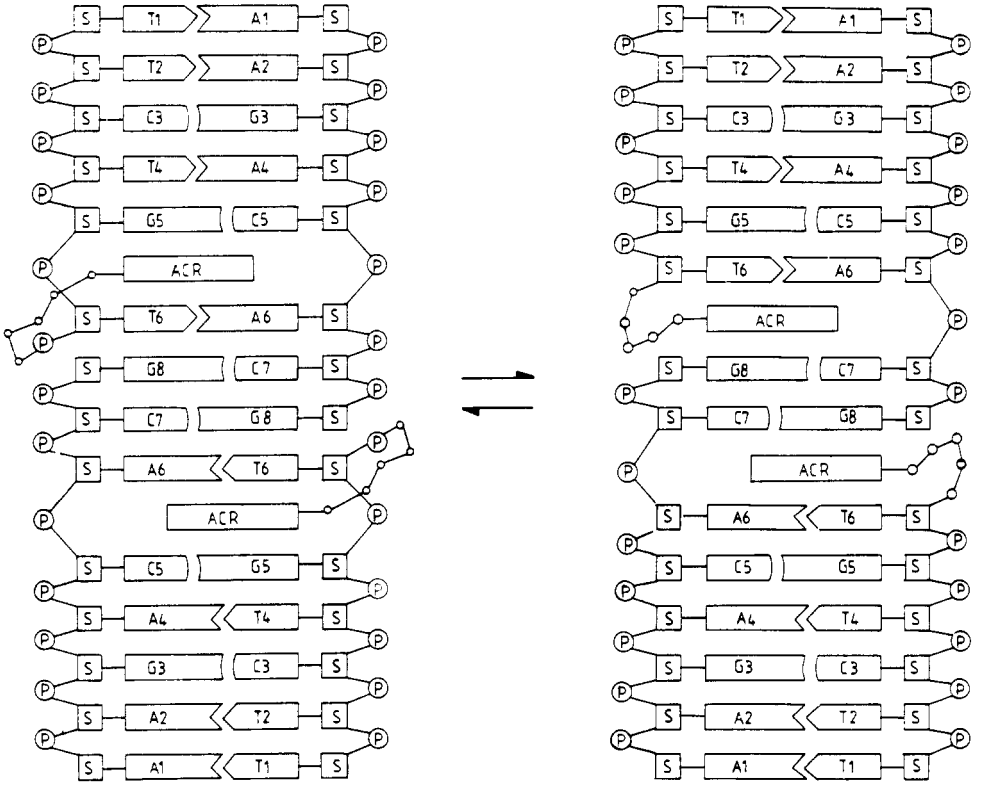

FIGURE 9: Model of the equilibrium between two conformations where the acridine dye is intercalated between the G_5-C_5 and the T_6-A_6 base pairs (model I) or sandwiched between the T_6-A_6 and the G_8-C_7 base pairs (model II) of two associated duplexes.

as suggested by the weakness of the NOE connectivities H_8-(G_5)-$H_{1'}$(T_6) and $H_8(G_5)$-$H_{2'}/H_{2''}(T_6)$ (Figures 4 and 5). As a matter of fact, the eight (or more) imino resonance lines observed at 5 °C can be due to slow exchange between the two complexes.

Building of a molecular Corey–Pauling–Koltren (CPK) model showed that a bridge with five methylene groups allowed intercalation of the acridine derivative between G_5-C_5 and T_6-A_6 base pairs. That the intercalating rings enter via the small groove of the double helix is shown by the NOE effect observed between $H_2(A_6)$ and H_7(Acr).

We conclude the presence of an equilibrium between two conformational families (Figure 9). In the first conformation, the acridine is stacked between G_5-C_5 and T_6-A_6 base pairs, while in the second conformation the acridine derivative is stacked between the T_6-A_6 base pair of the duplex and G_8-C_7 formed by the association of both duplexes. The first model is in agreement with the fact that only a very weak connectivity was observed between $H_8(G_5)$ and $H_6(T_6)$. The second model is in agreement with the fact that seven imino protons resonances are observed as expected in the symmetrical dimer (Figure 9), and we have observed a connectivity between $H_6(C_7)$ and $H_8(G_8)$. Moreover, NOE connectivities were observed between sugar protons of T_6 and acridine and between the H_2 proton of adenine A_6 and acridine dye.

The acridine rings can adopt two positions, depending on the rotation of the acridine moiety around the C_9–NH bond. In both positions the methylene groups were found close to protons of sugars belonging to the same strand. On the other hand, the formation of an asymmetric dimer, with the drug intercalated between G_5 and T_6 on one side and between T_6 and G_8 on the other, participating in the line broadening by exchange with the duplexes I and II cannot be excluded. The NOESY data do not exclude other structures that are not expected to lead to typical connectivities between the dye and the bases or the sugars. For example, the aromatic dye bears a positive charge at pH 7.0 and so can electrostatically bind to a phosphate group of the complementary sequence. This location of the aromatic dye is quite possible in CPK models of the complex.

Contrary to that observed on a tetramer duplex linked to an acridine derivative (Lancelot & Thuong, 1986), where both strands have the same number of bases, the studied duplex here has not shown any aggregation at room temperature. This peculiarity is due to the fact that, although the acridine dye is a hydrophobic species, the last two bases C_7 and G_8 of the complementary strand favor the formation of a duplex stabilized by the intercalation of the acridine.

When the temperature is lowered (<288 K), we suggest that the formation of a duplex dimer occurs, which thus includes two intercalated acridines, so that the superstructure corresponds to a tetradecamer of more than one helix turn. This then explains an increase of τ_{cr} (the correlation rotation time) leading to an increase in line width.

We identified each of the two isomers. Isomer I corresponds to the pseudoaxial configuration and isomer II to the pseudoequatorial configuration. Since several NOE effects were observed between sugar protons and the CH_2 of the neopentyl group of isomer I and not with isomer II, it has been concluded that the slight defect of stability of isomer I is due to a steric hindrance arising from the presence of the neopentyl group in the pseudoaxial isomer. Nevertheless, this steric hindrance did not induce significant changes in the duplex conformation since, except for the H_2 protons of adenine for which slight variations of the chemical shift were observed, the NMR spectra (1D and 2D) of both isomers were quite similar.

It is worth noting that, of the two isomers, the pseudoequatorial one, which forms the more stable duplex with its complementary sequence, was found to be the more resistant to the nucleases (Asseline et al., 1986b).

We conclude that these compounds which are more resistant to the nucleases than their diester analogues and which form stable complexes with their complementary sequence are more suitable for use in in vivo experiments than their natural homologues.

Registry No. (*R*)-d(T*TCTGT)m_5Acr·d(GCACAGAA), 112246-94-3; (*S*)-d(T*TCTGT)m_5Acr·d(GCACAGAA), 112418-56-1; (*R*)-d(T*TCTGT)m_5Acr, 112246-92-1; (*S*)-d(T*TCTGT)m_5Acr, 112344-63-5; (*R*)-d(T*TCTGT), 112219-69-9; (*S*)-d(T*TCTGT), 112295-36-0; 2-methoxy-6-chloro-9-aminoacridine, 3548-09-2.

References

Asseline, U., Delarue, M., Lancelot, G., Toulmé, F., Thuong, N. T., Montenay-Garestier, T., & Hélène, C. (1984a) *Proc. Natl. Acad. Sci. U.S.A. 81*, 3297–3301.

Asseline, U., Toulmé, F., Thuong, N. T., Delarue, M., Montenay-Garestier, T., & Hélène, C. (1984b) *EMBO J. 3*, 795–800.

Asseline, U., Thuong, N. T., & Hélène, C. (1986a) *Nucleosides Nucleotides 5*, 45–63.

Asseline, U., Barbier, C., & Thuong, N. T. (1986b) *Phosphorus Sulfur 26*, 63–73.

Barbet, J., Roques, B. P., Combrisson, S., & Le Pecq, J.-B. (1976) *Biochemistry 15*, 2642–2650.

Broido, M. S., Zon, G., & James, T. L. (1984) *Biochem. Biophys. Res. Commun. 119*, 663–670.

Brown, S. C., Mullis, K., Levenson, C., & Shafer, R. H. (1984) *Biochemistry 23*, 403–408.

Fazakerley, G. V., Guy, A., Téoule, R., Quignard, E., & Guschlbauer, W. (1985) *Biochimie 67*, 819–822.

Feigon, J., Leupin, W., Denny, W. A., & Kearns, D. R. (1983) *Biochemistry 22*, 5943–5951.

Feigon, J., Wang, A. H. J., van der Marel, G. A., van Boom, J. H., & Rich, A. (1984) *Nucleic Acids Res. 12*, 1243–1263.

Guittet, E., Piveteau, D., & Lallemand, J. Y. (1984) *Nucleic Acids Res. 12*, 5927–5941.

Hare, D. R., Wemmer, D. E., Chan, S. H., Drobny, G., & Reid, B. R. (1983) *J. Mol. Biol. 171*, 319–336.

Hélène, C., & Lancelot, G. (1982) *Prog. Biophys. Mol. Biol. 39*, 1–68.

Hore, P. J. (1983) *J. Magn. Reson. 55*, 283–300.

Hosur, R. V., Kumar, M. R., Roy, K. B., Zu-Kun, T., Miles, H. T., & Govil, G. (1985) in *Magnetic Resonance in Biology and Medicine* (Govil, G., Khetrapal, C. L., & Saran, A., Eds.) pp 243–260, Tata McGraw-Hill, New Dehli, India.

Lancelot, G., & Thuong, N. T. (1986) *Biochemistry 25*, 5357–5363.

Lancelot, G., Asseline, U., Thuong, N. T., & Hélène, C. (1985) *Biochemistry 24*, 2521–2529.

Marion, D., & Lancelot, G. (1984) *Biochem. Biophys. Res. Commun. 124*, 774–783.

Reid, D. G., Salisbury, S. A., & Williams, D. H. (1983) *Biochemistry 22*, 1377–1385.

Scheek, R. M., Russo, N., Boelens, R., Kaptein, R., & van Boom, J. A. (1983) *J. Am. Chem. Soc. 105*, 2914–2916.

Scheek, R. M., Boelens, R., Russo, N., van Boom, J. H., & Kaptein, R. (1984) *Biochemistry 23*, 1371–1376.

States, D. J., Haberkorn, R. A., & Ruben, D. J. (1982) *J. Magn. Reson. 48*, 286–292.

Stawinski, J., Hozumi, J., Naraug, S. A., Bachland, C. P., & Wu, R. (1977) *Nucleic Acids Res. 4*, 353–371.

Thuong, N. T., Chassignol, M., Lancelot, G., Mayer, R., Hartmann, B., Leng, M., & Hélène, C. (1981) *Biochimie 63*, 775–784.

Weiss, M. A., Patel, D. J., Sauer, R. T., & Karplus, M. (1984) *Proc. Natl. Acad. Sci. U.S.A. 81*, 130–134.

Wemmer, D. E., Chou, S.-H., Hare, D. R., & Reid, B. R. (1984) *Biochemistry 23*, 2262–2268.

Wemmer, D. E., Chou, S.-H., Hare, D. R., & Reid, B. R. (1985) *Nucleic Acids Res. 13*, 3755–3772.